Ionics (2017) 23:1399–1406
DOI 10.1007/s11581-016-1966-9

ORIGINAL PAPER

Ionic liquid-based electrolyte with dual-functional LiDFOB additive toward high-performance $LiMn_2O_4$ batteries

Bingsheng Qin[1] · Shu Zhang[1] · Zhenglin Hu[1] · Zhihong Liu[1] · Junnan Zhang[2] · Jianghui Zhao[1] · Junwei Xiong[3] · Guanglei Cui[1]

Received: 11 September 2016 / Revised: 12 December 2016 / Accepted: 27 December 2016 / Published online: 7 January 2017

Abstract Manganese oxide-based cathodes are one of the most promising lithium-ion battery (LIB) cathode materials due to their cost-effectiveness, high discharge voltage plateau (above 4.0 V vs. Li/Li^+), superior rate capability, and environmental benignity. However, these batteries using conventional $LiPF_6$-based electrolytes suffer from Mn dissolution and poor cyclic capability at elevated temperature. In this paper, the ionic liquid (IL)-based electrolytes, consisting of 1-butyl-1-methylpyrrolidinium bis(trifluoromethanesulfon)imidate ($PYR_{1,4}$-TFSI), propylene carbonate (PC), lithium bis(trifluoromethanesulfon)imide (LiTFSI), and lithium oxalyldifluoroborate (LiDFOB) additive, were explored for improving the high temperature performance of the $LiMn_2O_4$ batteries. It was demonstrated that LiTFSI-ILs/PC electrolyte associated with LiDFOB addition possessed less Mn dissolution and Al corrosion at the elevated temperature in $LiMn_2O_4$/Li batteries. Cyclic voltammetry and electrochemical impedance spectroscopy implied that this kind of electrolyte also contributed to the formation of a highly stable solid electrolyte interface (SEI), which was in accordance with the polarization measurement and the Li deposition morphology of the symmetric lithium metal cell, thus beneficial for improving the cycling performance of the $LiMn_2O_4$ batteries at the elevated temperature. Cyclic voltammetry and electrochemical impedance spectroscopy implied that the cells using this kind of electrolyte exhibited better interfacial stability, which was further verified by the polarization measurement and the Li deposition morphology of the symmetric lithium metal cell, thus beneficial for improving the cycling performance of the $LiMn_2O_4$ batteries at the elevated temperature. These unique characteristics would endow this kind of electrolyte a very promising candidate for the manganese oxide-based batteries.

Keywords Ionic liquid-based electrolyte · $LiMn_2O_4$ batteries · Dual-functional additive · Solid electrolyte interface

Bingsheng Qin and Shu Zhang contributed equally to this work.

Electronic supplementary material The online version of this article (doi:10.1007/s11581-016-1966-9) contains supplementary material, which is available to authorized users.

✉ Zhihong Liu
liuzh@qibebt.ac.cn

✉ Guanglei Cui
cuigl@qibebt.ac.cn

[1] Qingdao Industrial Energy Storage Research Institute, Qingdao Institute of Bioenergy and Bioprocess Technology, Chinese Academy of Sciences, Qingdao 266101, People's Republic of China

[2] Research Institute of Technology, Shandong WINA Green Power Technology Co., Ltd., Weifang 262700, People's Republic of China

[3] Key Laboratory for Liquid-Solid Structural Evolution & Processing of Materials (Ministry of Education), Shandong University, Jinan 250061, People's Republic of China

Introduction

In the past two decades, lithium-ion batteries have played successful role in the consumable electronic device markets [1, 2]. Very recently, the rapid growth of electrical vehicles (EV) and renewable energy such as wind and solar power spurs the large-format applications of lithium-ion batteries. To aim at these large-scale applications, it is imperative to seek higher energy devices along with lower cost and environmental benignity [3, 4]. Although Li-O_2 and Li-S batteries could deliver higher energy density more than 300 Wh kg^{-1}, there are still some key challenges waiting for suitable solutions before successful commercialization [5, 6]. The Na-ion batteries are also regarded as promising low-cost energy storage

devices with considerable energy density. However, their research and development are just in the beginning stage. As a compromise, the batteries with lithium metal anode and high voltage cathodes are demonstrated to provide a medium energy density of around 250 Wh kg^{-1} with low cost in the near future [7–9]. Manganese oxide-based cathodes ($LiNi_xCo_yMn_zO_4$) including lithium-rich manganese-based material (Li_2MnO_3-$LiMO_2$) are one of the most promising lithium-ion battery (LIB) cathode materials due to their cost-effectiveness, high discharge voltage plateau (above 4.0 V vs. Li/Li^+), superior rate capability, and environmental benignity [10–12]. However, manganese oxide-based batteries using conventional $LiPF_6$-based electrolytes suffered from poor cyclic capability at the elevated temperature above 55 °C [13, 14]. This drawback originated from the thermal instability of $LiPF_6$ salt, which readily decomposed into HF, LiF, and PF_5 at elevated temperature or with even trace of water [15, 16]. The HF would erode the cathode and cause the Mn dissolution into the electrolyte, while PF_5 could react with the carbonate solvents. The dissolved Mn ions migrate to anode and are reductively deposited on the anode surface resulting in increased impedance [14, 17]. Therefore, tailoring a high-performance electrolyte is of significant importance for large-scale applications of $LiNi_xCo_yMn_zO_4$ batteries.

We have been researching for the high-performance electrolytes to improve the high temperature performance of manganese oxide-based batteries [13, 18]. For simplicity, we take $LiMn_2O_4$ battery as a model for better explanation and understanding. In our previous report, a single-ion gel polymer electrolyte (polymeric lithium tartaric acid borate @ poly(vinylidene fluoride-co-hexafluoropropylene) was already explored for improving the cycling performance of $LiMn_2O_4$-based lithium battery at the elevated temperature owing to its superior thermal stability [13]. Herein, the ionic liquid (IL)-based electrolytes were investigated for attempting high performance of manganese oxide-based batteries at elevated temperature. Owing to their non-flammability, negligible vapor pressure, and high thermal stability, ionic liquid-based electrolytes have drawn extensive attention for energy storage applications [19, 20]. Among them, lithium bis(trifluoromethanesulfon)imide (LiTFSI) and PYR_{14}TFSI electrolyte was featured by favorable conductivity and superior thermal and electrochemical stability, making it a kind of very promising electrolyte toward LIB applications. Recently, it was reported that the addition of a co-solvent with a reasonable amount solvent such as PC could effectively lower its viscosity so as to improve the ionic conductivity and simultaneously maintain the superior electrochemical stability as well as the flame retardant performance [21–23]. However, most of the previous reports focused on the design and characterization of the IL electrolytes mainly based on the stable $LiFePO_4$ electrode system. Up to now, only very few reports are available to employ them in the manganese oxide-based electrode materials to address their instability issues both thermally and electrochemically in conventional organic carbonate electrolytes [24–26]. Especially, the rational design of an ionic liquid-based electrolyte with co-solvent and additive in the commercialized $LiMn_2O_4$ batteries was never systematically reported before.

In this paper, LiTFSI-ILs/PC electrolytes along with tailored functional additive were systematically characterized and fully discussed for the first time to improve the performance of commercially available manganese oxide-based batteries.

Experimental

Materials

$PYR_{1,4}$-TFSI (99 %, Shanghai Chengjie Chemical Co., Ltd.), LiTFSI and 1 M $LiPF_6$-EC/DMC (1/1, *v*/*v*) (Guotai-huarong New Chemical Materials Co., Ltd.), LiDFOB (≥99 %, Suzhou Fosai Co., Ltd.), $LiMn_2O_4$ (Hunan Reshine New Material Co., Ltd.), lithium sheets (≥99.9 %, China Energy Lithium Co., Ltd.), propylene carbonate (PC, Capchem Technology Co., Ltd), and PP separator (Celgard 2500). All materials were commercially available and used without further purification.

Preparation of ionic liquid-based electrolytes

$PYR_{1,4}$-TFSI and PC were mixed by the ratio of 7:3 (*w*/*w*) to prepare 0.3 M LiTFSI-ILs/PC electrolyte. At this ratio of ILs/PC, the electrolyte could deliver both decent ionic conductivity and flame retardant ability based on our optimization [21–23]. LiDFOB additive (2 wt%) was added to the electrolyte to enhance the battery performance.

Electrochemical characterization of the electrolyte

The electrochemical stability of the electrolytes at room temperature was evaluated by the linear sweep voltammetry (LSV) method performed on a stainless steel working electrode and a lithium metal foil counter electrode at a scanning rate of 0.5 mV s^{-1}. Inert stainless steel electrode was usually used as a working electrode for the LSV tests instead of active electrode [27]. The ionic conductivity of the three electrolytes (EC/DMC-$LiPF_6$, LiTFSI-ILs/PC, and LiTFSI-ILs/PC with 2 % LiDFOB additive) with PP separators was measured between two stainless steel plate electrodes and calculated by the formula as follows:

$$\sigma = \frac{L}{SR}$$

In this formula, L stands for the thickness of the PP separator, S stands for the area of the stainless steel electrode, and R is the resistance of the electrolyte, which can be obtained by

the AC impedance analysis using a Zahner Zennium electrochemical workstation over a frequency range of 0.1–10^6 Hz with perturbation amplitude of 10 mV.

Cells assembly and performance

The Li/$LiMn_2O_4$ cells (2032-type) were assembled by sandwiching the electrolytes between lithium metal foils and $LiMn_2O_4$ electrodes, respectively. The $LiMn_2O_4$ electrode was composed of 90 wt% $LiMn_2O_4$ (around 3.0 mg active material on 1.54 cm^2 aluminum metal foil), 5 wt% PVDF, and 5 wt% carbon black. Symmetric lithium metal cells (2032-type) assembled by sandwiching the electrolytes between two lithium metal foils were used for polarization measurements. The separator used here is Celgard 2500 (polypropylene), and the volume of the electrolyte used for each cell was fixed at 120 μL. At least two cells were made in parallel for each test to obtain consistent cell performance. Each cell was rested for 8 h before test.

All assembly of cells was carried out in an argon-filled glove box (H_2O content <0.1 ppm, O_2 content <0.1 ppm). The charge/discharge profiles and cycling performance of cells were recorded on a LAND battery test system. The galvanostatic charge/discharge behaviors of the $LiMn_2O_4$/Li batteries were conducted at a constant current density of 0.195 mA cm^{-2} over the range of 3.0~4.3 V. The polarization measurement of the symmetric Li/Li batteries was conducted by a constant deposition/dissolution current density of 0.2 mA cm^{-2}. The AC impedance of the cells after 1st and 100th cycle and the variation in electrode polarization during cycling at the elevated temperature were measured by the methods mentioned above. The surface morphology of lithium metal foils and $LiMn_2O_4$ cathodes after cycling was observed by Hitachi S-4800 field emission scanning electron microscope (SEM). After the cells were cycled for 100 cycles at elevated temperatures, the electrolyte was carefully collected and rinsed in 10 mL concentrated HNO_3 solution. The obtained solution was then diluted by 1000 times before the Mn and Al element concentrations were evaluated by the inductively coupled plasma mass spectrometry (ICP-MS, Thermo X7, limit of detection (LOD) = 0.5 ppm).

Results and discussions

Electrochemical stability of the electrolytes

The electrochemical stability requires the electrolyte to be resistant for electrochemical reduction and oxidation while cycling, which is one of the important parameters of the electrolyte [28]. As depicted in Fig. 1, the $LiPF_6$-based electrolyte started to oxidatively decompose at about 4.5 V vs. Li/Li^+ at room temperature, which was in accordance with previous report [29]. By contrast, the LiTFSI-ILs/PC electrolyte started anodic oxidization up to 4.8 V vs. Li/Li^+, which was slightly higher than that of $LiPF_6$-based electrolyte. This could be ascribed to the better electrochemical stability of $PYR_{1,4}$-TFSI and PC [21, 30]. Interestingly, when 2 wt% LiDFOB additive was added into the LiTFSI-ILs/PC electrolyte, the electrochemical stability was further enhanced to 5.3 V vs. Li/Li^+, which was higher than that of some classical electrolytes [28]. It is well known that the electrochemical stability determined by linear sweep voltammetry greatly depends on both thermodynamic and kinetic factors. According to previous literatures [28, 29], we speculated that the addition of 2 % LiDFOB into LiTFSI-ILs/PC electrolyte could result in more stable interface kinetically thus increasing the electrochemical stability. This superior electrochemical stability of the IL-based electrolytes could better qualify the operating of the $LiMn_2O_4$ batteries over the voltages 3.0–4.3 V.

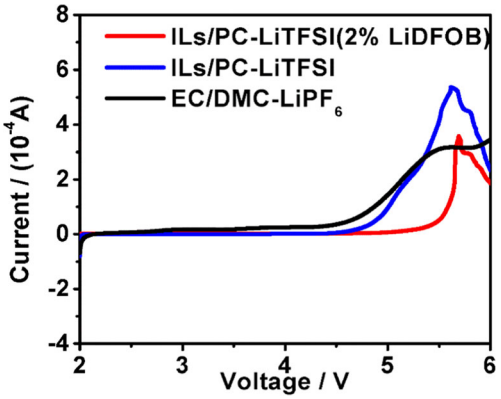

Fig. 1 Linear sweep voltammetry comparison of the three electrolytes: EC/DMC-$LiPF_6$, LiTFSI-ILs/PC, and LiTFSI-ILs/PC with 2 % LiDFOB as additive (scan rate = 0.5 mV s^{-1})

Ionic conductivity and flame retardance performance of the electrolytes

Ionic conductivity is another critical parameter for a new electrolyte [28, 31]. As shown in Fig. 2, all the electrolytes

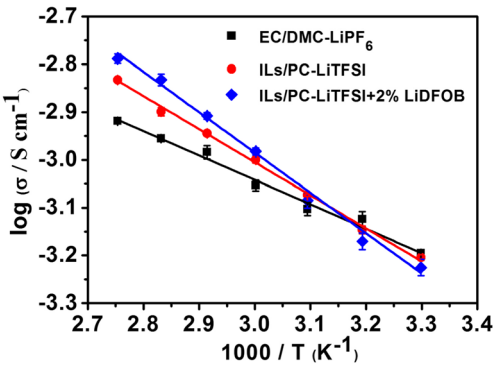

Fig. 2 Temperature dependence of the ionic conductivity of the three electrolytes with separators: EC/DMC-$LiPF_6$, LiTFSI-ILs/PC, and LiTFSI-ILs/PC with 2 % LiDFOB as additive

featured favorable ionic conductivity for practical application over the temperature range between 30 and 80 °C. Besides, the ionic conductivity vs. temperature relationships agreed quite well with the Arrhenius equation over the temperature range. It was noted that the EC/DMC-$LiPF_6$ electrolyte exhibited higher ionic conductivity at relatively low temperatures compared to that of the ionic liquid-based electrolytes. This is because the ionic liquid-based electrolytes had higher viscosity at the relatively low temperatures restraining the ionic motion. However, when the temperature was increased to be higher than 50 °C, the ionic conductivity of the ionic liquid-based electrolytes became higher than that of the EC/DMC-$LiPF_6$ electrolyte. This is mainly due to that the viscosity of the IL electrolytes was much alleviated at elevated temperatures, which was no longer a limiting effect on ionic transportation [21]. Besides, for security reasons, the EC/DMC-$LiPF_6$ electrolyte is generally not used at a temperature higher than 55 °C. When the temperature was increased above 70 °C, the ionic conductivity of the IL electrolyte with LiDFOB addition was slightly higher than that of the electrolyte without addition. This can be explained by the fact that LiDFOB is a highly dissociated lithium salt, and its addition to the electrolyte could increase the ionic concentrations and enhance the ionic conductivity to some extent. It was also manifested in our work that the IL-based electrolytes were difficult to be ignited or subsequently self-extinguished very soon (see Fig. S1). As a comparison, the EC/DMC-$LiPF_6$-based electrolyte was well known to be highly flammable. As a conclusion, the IL-based electrolytes were much safer compared with the EC/DMC-$LiPF_6$ electrolyte.

The cycling performance of $LiMn_2O_4$ batteries

To verify the feasibility of the IL-based electrolytes in LIB applications, the $LiMn_2O_4$/Li battery performance was evaluated. It was shown in Fig. 3 that the specific capacity profiles vs. cycle number for the $LiMn_2O_4$ batteries using different electrolytes at room temperature and at the elevated temperature of 55 °C, respectively. At room temperature, the cell using the EC/DMC-$LiPF_6$ electrolyte possessed an initial specific capacity of 100.4 mAh g^{-1}. After 100 cycles, the specific capacity faded to 92.3 mAh g^{-1} with a capacity retention ratio of 91.9 %, indicating that the $LiMn_2O_4$ batteries using the EC/DMC-$LiPF_6$ electrolyte presented stable cycling performance at room temperature. The cell using 0.3 M LiTFSI-ILs/PC electrolyte exhibited a specific capacity fading from 100.0 to 93.3 mAh g^{-1} with a retention ratio of 93.3 % after 100 cycles. For the $LiMn_2O_4$ batteries using LiTFSI-ILs/PC electrolyte with 2 % LiDFOB, the capacity retention was slightly improved up to 95.6 % (from 99.5 to 95.1 mAh g^{-1}). This result indicated that LiDFOB played a positive role in improving the cell performance at room temperature. Above all, these results demonstrated that the $LiMn_2O_4$ batteries using these three kinds of electrolytes displayed comparable cycling performance at room temperature.

In sharp contrast, the cycling performance deviation for the cells using different electrolytes became more pronounced at elevated temperature of 55 °C. As depicted in Fig. 3b, the EC/DMC-$LiPF_6$-based cell underwent rapid capacity deterioration from 100.5 to 73.6 mAh g^{-1} with a capacity retention ratio of 73.2 %, which had the similar tendency to the previous literature and this could be well explained by the severe $LiMn_2O_4$ cathode corrosion in this $LiPF_6$-based electrolyte [14]. The cell using 0.3 M LiTFSI-ILs/PC electrolyte exhibited a relatively slow fading rate from 98.5 to 90.3 mAh g^{-1} at the beginning 35 cycles; however, it experienced a rather rapid capacity fading in the following circles indicative of a sudden internal breakdown or failure in the cell. It was hypothesized that the Al current collector was corroded by LiTFSI salt, and this process was accelerated at the elevated temperature, which caused a gradual structural collapse or increased impedance of the cell [23]. In this regard, some evidence will be offered by SEM and ICP-MS measurement and discussed later. By contrast, the cell using ILs/PC electrolyte with 2 % LiDFOB addition possessed the best capacity retention of 90 % after 100 cycles indicating extremely limited Al corrosion and $LiMn_2O_4$ cathode corrosion occurred in this system. This result implied that the LiDFOB additive could effectively suppress the Al corrosion caused by $TFSI^-$ due to the formation of a stable boron-containing compound on the surface of the current collector as reported in other literature [32].

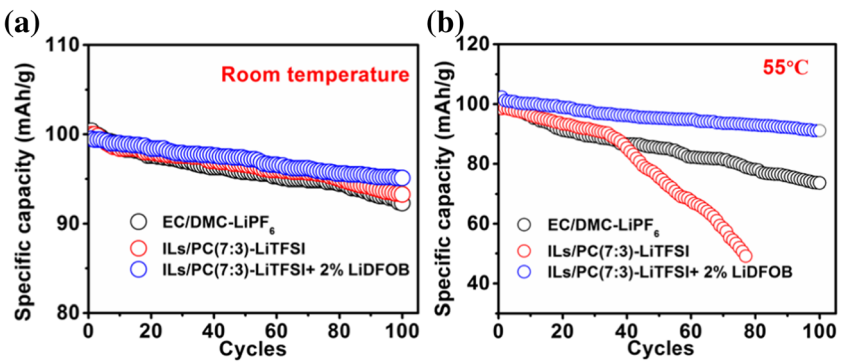

Fig. 3 Cyclic performance of $LiMn_2O_4$ batteries for the three electrolytes (**a**) at room temperature and (**b**) at the elevated temperature of 55 °C, respectively

SEM and ICP-MS analysis

SEM and ICP-MS measurements were conducted to gain a deep insight of the above different battery performance. Figure 4a–h showed the SEM image comparison of the lithium metal foil electrodes and $LiMn_2O_4$ electrodes before and after long-term cycling in different electrolytes at 55 °C, respectively. It was shown that the SEM image of the pristine lithium electrode exhibited a smooth surface. However, after cycling in the EC/DMC-$LiPF_6$ electrolyte, the lithium foil surface became rather rough and was composed of a large amount of lithium dendrites, which was in accordance with other EC/DMC-$LiPF_6$ electrolyte-based batteries [33, 34]. In sharp comparison, for the lithium electrode cycled in both IL-based electrolytes, no obvious rough dendrites were observed. In addition, the $LiMn_2O_4$ electrode after long-term cycling in IL-based electrolytes both with and without LiDFOB addition showed a similar morphology to the pristine $LiMn_2O_4$ electrode. However, the $LiMn_2O_4$ electrode surface in EC/DMC-$LiPF_6$ electrolyte displayed some cracks among the particles, demonstrating that it was seriously corroded in such electrolyte. According to previous reports, this corrosion was caused by HF, originated from the thermal decomposition of the $LiPF_6$ salts at elevated temperatures [14]. These SEM observations verified that the ionic liquid-based electrolytes had excellent compatibility with lithium foil anode and $LiMn_2O_4$ cathodes during battery cycling at the elevated temperature.

In order to obtain a full understanding of these Mn and Al corrosion phenomena, we performed ICP-MS measurement to evaluate the Mn and Al concentrations in these three electrolytes after 100 cycles at the temperature of 55 °C. As depicted in Table S1, the cells using IL-based electrolytes both with and without additive featured by very limited Mn dissolution (<0.5 and 0.9 ppm, respectively) compared to the cells using EC/DMC-$LiPF_6$ electrolyte (8.9 ppm), meaning that the $LiMn_2O_4$ cathode corrosion was highly alleviated in the IL-based electrolytes owing to their superior thermal and electrochemical stability. Note that the Mn dissolution in the LiTFSI-ILs/PC electrolyte with 2 % LiDFOB addition was even less compared to that without additive, which was in good accordance with its better performance both at room temperature and at elevated temperature of 55 °C as mentioned before. This finding further indicated that the LiDFOB additive played a positive role in suppressing the Mn dissolution and improving the interfacial stability. The Al element concentration in the 0.3 M LiTFSI-ILs/PC electrolyte was 5.5 ppm, which was much higher than that in the EC/DMC-$LiPF_6$ electrolyte and the IL with 2 % LiDFOB additive (both <0.5 ppm). The higher Al content in electrolyte should be unambiguously ascribed to the Al current collector corrosion caused by $TFSI^-$ anion, which was speculated to be responsible for the rapid capacity fading during the battery cycling at 55 °C. From another point of view, it proved that the addition of 2 % LiDFOB could effectively suppress the Al corrosion in the LiTFSI-based electrolyte. Overall, these findings demonstrated that LiTFSI-ILs/PC electrolyte associated with LiDFOB as a multifunctional additive possessed less Mn dissolution and Al corrosion at the elevated temperature in $LiMn_2O_4$-based batteries.

Polarization measurements and the Li deposition morphologies of the symmetric Li/Li batteries

Polarization measurements and the Li deposition morphologies of the symmetric Li/Li batteries were conducted to understand the effect of three different kinds of electrolytes on stabling the interface between the Li metal and electrolyte. During this experiment, a constant deposition/dissolution current density of 0.2 mA cm^{-2} was passed through the Li/Li cells for 100 h at 55 °C. The EC/DMC-$LiPF_6$ electrolyte

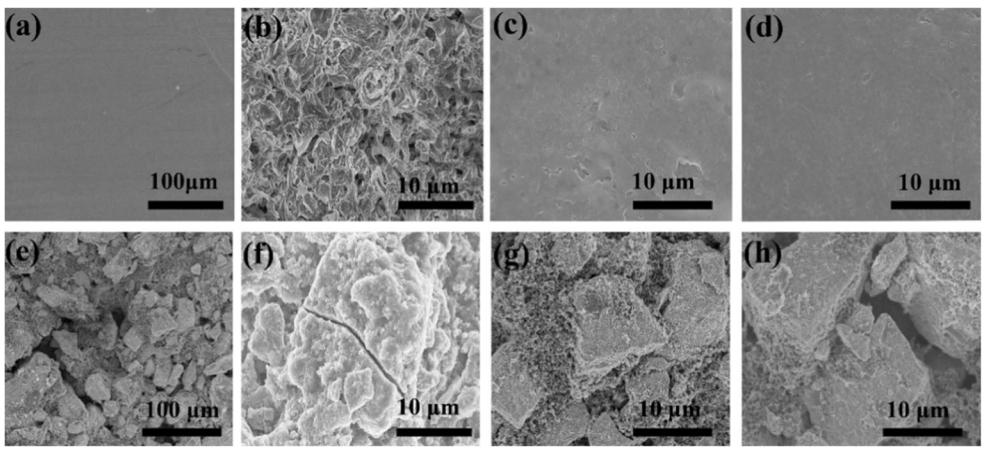

Fig. 4 Typical SEM images of the pristine lithium foil anode (**a**), the lithium anodes for EC/DMC-$LiPF_6$ electrolyte (**b**), 0.3 M LiTFSI-ILs/PC electrolyte (**c**), 0.3 M LiTFSI-ILs/PC electrolyte with 2 % LiDFOB addition (**d**), and the pristine $LiMn_2O_4$ cathode (**e**), the $LiMn_2O_4$ cathode for EC/DMC-$LiPF_6$ electrolyte (**f**), 0.3 M LiTFSI-ILs/PC electrolyte (**g**), and 0.3 M LiTFSI-ILs/PC electrolyte with 2 % LiDFOB addition (**h**) after 100 cycles in Li/$LiMn_2O_4$ batteries at 55 °C, respectively

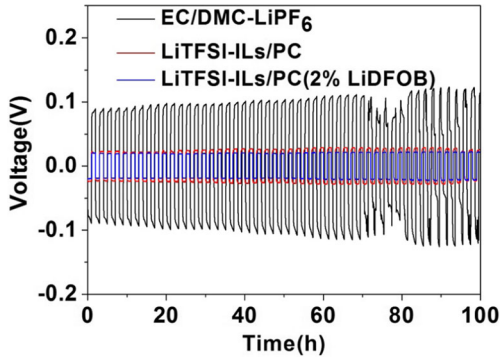

Fig. 5 Galvanostatic voltage–time curves respectively in EC/DMC-$LiPF_6$, LiTFSI-ILs/PC and LiTFSI-ILs/PC with 2 % LiDFOB electrolytes at 55 °C. The constant current density was 0.2 mA cm^{-2}

system showed the largest over-voltage among three electrolytes and an ascending tendency with time (Fig. 5), which was consistent with previous report [35]. The over-voltage of the LiTFSI-ILs/PC electrolyte was more stable with a slight increase, while the LiTFSI-ILs/PC electrolyte with 2 % LiDFOB addition showed excellent Li deposition/dissolution performance with the lowest over-voltage.

Figure 6 showed the SEM images of the Li foils surface harvested from the symmetric Li/Li batteries with different electrolytes after 100 hs galvanostatic cycling at 55 °C. In EC/DMC-$LiPF_6$ electrolyte, the loose dendritic structure was found on the Li surface, which was observed in previous report [35], while in the LiTFSI-ILs/PC electrolyte and the LiTFSI-ILs/PC electrolyte with 2 % LiDFOB addition showed smooth and compact morphology, especially the latter. It was indicated that the LiTFSI-ILs/PC electrolyte with 2 % LiDFOB addition can stabilize Li deposition and suppress the growth of lithium dendrites. The differences in the over-voltages and Li deposition morphologies with different electrolytes were associated with the solid electrolyte interface. As reported before, $TFSI^-$ decomposes to F^- [36] and then LiF, used as an additive to stable the SEI film of lithium metal anode [35] [37], forms on the anode surface. So the existence of $TFSI^-$ would make a uniform deposition of lithium. Furthermore, LiDFOB is also used as additive to improve the stability of lithium-ion battery [38] [39]. Combined with these reports and our experiment, it can be speculated that LiTFSI-ILs/PC electrolyte with 2 % LiDFOB addition was in favor of forming stable interface on Li anode.

Cyclic voltammetry and AC impedance analysis for the $LiMn_2O_4$ batteries

To gain a deep insight of the excellent cycling performance of the LiTFSI-ILs/PC electrolyte with 2 % LiDFOB for the $LiMn_2O_4$ batteries, the variation of the electrode polarization during long-term cycling at elevated temperature of 55 °C was measured using cyclic voltammetry method (Fig. 7a, b) where the EC/DMC-$LiPF_6$ based cell was used as the control sample. The cells were tested at a scan rate of 0.2 mV s^{-1} over a voltage range of 3.4–4.6 V. In cyclic voltammetry, the variation of peak currents and potential separations of the redox peaks were known to indicate different kinetics during battery cycling [13]. In the case of EC/DMC-$LiPF_6$ electrolyte-based $LiMn_2O_4$ battery, the peak current faded dramatically from 2.10 mA (after 1st cycle) to 0.66 mA (after 100th cycle) (ΔI = 1.44 mA) and the potential separation increased from 0.11 V (after 1st cycle) to 0.35 V (after 100th cycle) (ΔV = 0.24 V). These gaps of peak currents and potential separations indicated that continuous side reactions occurred within the interfaces during battery cycling. In comparison, the peak currents for the LiTFSI-ILs/PC with 2 % LiDFOB electrolyte were slightly reduced from 1.82 mA (after 1st cycle) to 1.68 mA (after 100th cycle) (ΔI = 0.14 mA) and almost no potential separation growth was observed during the 100 charge/discharging cycles. The quantitative comparison of these results undoubtedly confirmed that the IL-based electrolyte tailored by LiDFOB additive contributed to form a highly stable SEI.

In addition to the above CV argument, the AC impedance analyses of the cells after the 1st and 100th cycle were conducted (depicted in Figs. 7c, d and S3). According to previous reports [40–42], there were two semicircles in the high-frequency region representing the solid electrolyte interface and the charge-transfer process respectively and a straight line in the low-frequency region representing the Warburg diffusion in the EIS spectra of the $LiMn_2O_4$/Li cell with organic electrolyte at discharged state at 55 °C. For ionic liquid-based cells, the other semicircle was apparent which represented the impedance of the SEI layer in this system. This unique phenomenon was observed after the first discharge, demonstrating that the ionic liquid electrolyte used here might promote the formation of solider SEI layer at elevated temperature of 55 °C with the use of the LiDFOB additive. The impedance spectra were fit with an equivalent circuit [41, 42], and the results were shown in Fig. S3. The charge-transfer impedance with the EC/DMC-$LiPF_6$ electrolyte increased much from 35.49 Ω (1st cycle) to 214.70 Ω (100th cycle), indicating a huge internal resistance growth within the interfaces between the electrolyte and the electrodes during battery cycling. By contrast, the cell impedance based on the LiTFSI-ILs/PC electrolyte with LiDFOB addition was slightly increased from 59.42 Ω for 1st cycle to 106.20 Ω after 100th cycles, indicating that the growth of cell impedance was significantly suppressed. These findings implied that the ionic liquid-based electrolyte with LiDFOB addition could help build a more stable SEI between the electrolyte and the electrodes during battery cycling, thus beneficial for improving the cycling performance of the $LiMn_2O_4$/Li batteries at the elevated temperature.

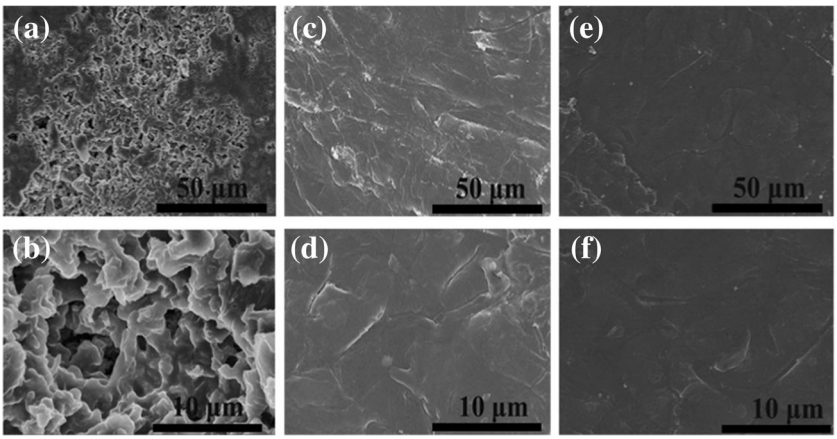

Fig. 6 SEM images of Li surface after 100 h galvanostatic cycling in Li/Li symmetric cells with a constant current density of 0.2 mA cm^{-2} at 55 °C. **a**, **b** For the EC/DMC- $LiPF_6$ electrolyte, **c**, **d** for the LiTFSI-ILs/PC electrolyte, and **e**, **f** for the LiTFSI-ILs/PC with 2 % LiDFOB electrolyte, respectively

The modified Voigt-FMG equivalent circuit proposed by Aurbach and co-workers [12, 13] was successfully used to simulate the whole range of insertion potentials of the lithiated graphite electrode as an anode material for lithium-ion batteries, and the kinetic parameters were obtained by simulation, including surface film capacitance (Cf) and resistance for Li+ migration through the surface film (Rf), charge-transfer resistance at the bulk-electrolyte interface (Rct), double-layer capacitance (Cdl), diffusion coefficient reflecting the diffusion of Li^+ in the solid phase (DLi), and insertion capacitance reflecting the occupation of Li^+ into the inserted sites (Cint). This equivalent circuit was believed to be suitable also for describing the process of Li+ insertion into transition metal oxides, such as $LiMn_2O_4$, $LiMnO_2$, $LiNiO_2$, and $LiCoO_2$.

Conclusion

In summary, LiTFSI-ILs/PC-based electrolytes with addition of 2 % LiDFOB exhibited superior electrochemical stability and considerable ionic conductivity when compared with commercially available EC/DMC-$LiPF_6$ electrolyte. The $LiMn_2O_4$/Li cells using this kind of electrolyte exhibited excellent cycling performance at the elevated temperature of 55 °C. It was demonstrated that LiTFSI-ILs/PC electrolyte associated with LiDFOB addition possessed less Mn dissolution and Al corrosion at the elevated temperature in $LiMn_2O_4$/Li batteries. CV and AC impedance analysis also implied that this kind of electrolyte contributed to form a highly stable solid electrolyte interface, which was consistent with polarization measurements and the Li deposition morphologies of the symmetric Li/Li batteries, thus beneficial for improving

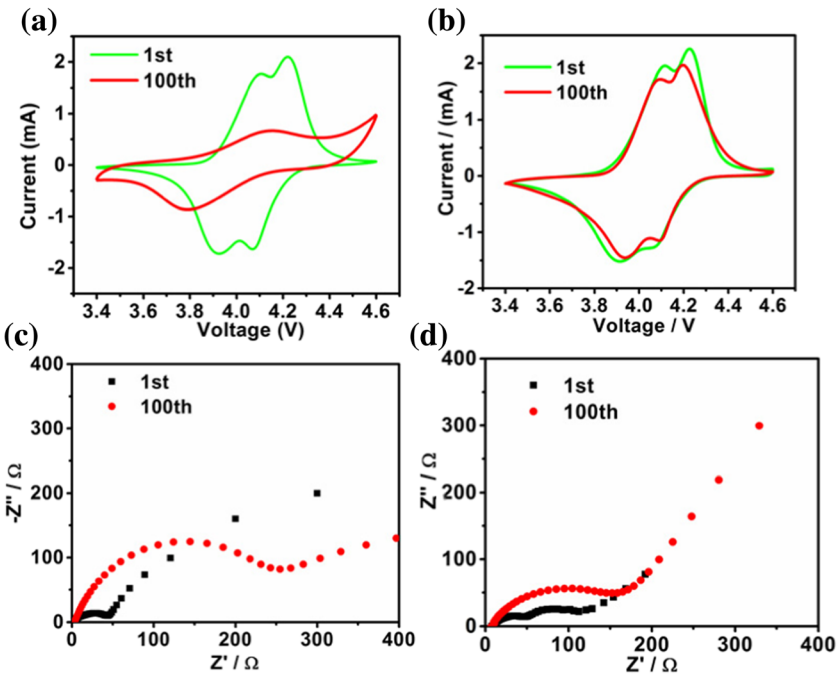

Fig. 7 Cyclic voltammograms and AC impedance analysis of the $LiMn_2O_4$/Li batteries using EC/DMC-$LiPF_6$ electrolyte (**a**, **c**) and LiTFSI-ILs/PC with 2 % LiDFOB electrolyte (**b**, **d**) after the 1st and 100th cycle at the elevated temperature of 55 °C, respectively

the cycling performance of the $LiMn_2O_4$/Li batteries at elevated temperatures. These unique characteristics would endow this kind of electrolyte be a very promising electrolyte for the manganese oxide-based batteries.

Acknowledgements This work was supported by the National Program on the National High Technology Research and Development Program of China (863 program, No. 2013AA050905), Key Project of Natural Science Foundation of Shandong Province (ZR2015QZ01), "135" Projects Fund of CAS-QIBEBT Director Innovation Foundation, and Qingdao Institute of Bioenergy and Bioprocess Technology Director Technology Foundation.

References

1. Goodenough JB, Park KS (2013) J Am Chem Soc 135:1167
2. Ritchie A, Howard W (2006) J Power Sources 162:809
3. Dunn B, Kamath H, Tarascon J-M (2011) Science 334:928
4. Thackeray MM, Wolverton C, Isaacs ED (2012) Energy Environ. Sci. 5:7854
5. Bresser D, Passerini S, Scrosati B (2013) Chem Commun 49:10545
6. Bruce PG, Freunberger SA, Hardwick LJ, Tarascon J-M (2012) Nat Mater 11:19
7. A. M, Tarascon J-M (2001) Nature 414:9
8. Scrosati B, Garche J (2010) J Power Sources 195:2419
9. Scrosati B, Hassoun J, Sun Y-K (2011) Energy Environ. Sci. 4:3287
10. Sun Y-K, Lee Y-S, Yoshio M, Amine K (2002) Electrochem Solid-State Lett 5:A99
11. Ammundsen B, Paulsen J (2001) Adv Mater 13:943
12. Desilvestro J, Haas O (1990) J Electrochem Soc 137:5C
13. Qin B, Liu Z, Ding G, Duan Y, Zhang C, Cui G (2014) Electrochim Acta 141:167
14. Xu G, Liu Z, Zhang C, Cui G, Chen L (2015) J Mater Chem A 3: 4092
15. Botte GG, White RE, Zhang Z (2001) J Power Sources 97–98:570
16. Kawamura T, Okada S, Yamaki J-i (2006) J Power Sources 156:547
17. Sun Y-K, Myung S-T, Park B-C, Prakash J, Belharouak I, Amine K (2009) Nat Mater 8:320
18. Hu P, Duan Y, Hu D, Qin B, Zhang J, Wang Q, Liu Z, Cui G, Chen L (2015) ACS Appl Mat Interfaces 7:4720
19. Shin J-H, Henderson WA, Passerini S (2003) Electrochem Commun 5:1016
20. Gebresilassie Eshetu G, Armand M, Scrosati B, Passerini S (2014) Angew Chem Int Ed 53:13342
21. Kühnel RS, Böckenfeld N, Passerini S, Winter M, Balducci A (2011) Electrochim Acta 56:4092
22. Kühnel R-S, Balducci A (2014) J Phys Chem C 118:5742
23. Kühnel R-S, Lübke M, Winter M, Passerini S, Balducci A (2012) J Power Sources 214:178
24. Gao X-W, Feng C-Q, Chou S-L, Wang J-Z, Sun J-Z, Forsyth M, MacFarlane DR, Liu H-K (2013) Electrochim Acta 101:151
25. Swiderska-Mocek A (2014) J Solid State Electrochem 18:1077
26. Wongittharom N, Lee T-C, Hung IM, Lee S-W, Wang Y-C, Chang J-K (2014) J Mater Chem A 2:3613
27. Hofmann A, Werth F, Howeling A, Hanemann T (2015) ECS Electrochem Lett 4:A141
28. Xu K (2004) Chem Rev 104:116
29. Qin B, Liu Z, Zheng J, Hu P, Ding G, Zhang C, Zhao J, Kong D, Cui G (2015) J Mater Chem A 3:7773
30. Menne S, Kühnel RS, Balducci A (2013) Electrochim Acta 90:641
31. Park M, Zhang X, Chung M, Less GB, Sastry AM (2010) J Power Sources 195:7904
32. Park K, Yu S, Lee C, Lee H (2015) J Power Sources 296:197
33. Miao R, Yang J, Feng X, Jia H, Wang J, Nuli Y (2014) J Power Sources 271:291
34. Xu W, Wang J, Ding F, Chen X, Nasybulin E, Zhang Y, Zhang J-G (2014) Energy Environ Sci 7:513
35. Lu Y, Xu S, Shu J, Aladat WIA, Archer LA (2015) Electrochem Commun 51:23
36. Leroy S, Martinez H, Dedryvere R, Lemordant D, Gonbeau D (2007) App Surf Sci 253:4895
37. Choudhury S, Archer LA (2016) Adv Electron Mater 2:1500246
38. Chen Z, Qin Y, Liu J, Amine K (2009) Electrochem Solid-State Lett 12:A69
39. Xu M, Zhou L, Hao L, Xing L, Li W, Lucht BL (2011) J Power Sources 196:6794
40. Xia Y, Zhou Y, Yoshio M (1997) J Electrochem Soc 144:2593
41. Lu D, Li W, Zuo X, Yuan Z, Huang Q (2007) J Phys Chem C 111: 12067
42. Levi MD, Aurbach D (1997) J Phys Chem B 101:4630